P5.14 ADVANCED TORNADO DETECTION ALGORITHM USING SUPER-RESOLUTION AND POLARIMETRIC DATA

Yadong Wang[1,2,*] and Tian-You Yu[1,2]

[1] School of Electrical and Computer Engineering, University of Oklahoma, Norman, Oklahoma, USA
[2] Atmospheric Radar Research Center, University of Oklahoma, Norman, Oklahoma, USA

1. INTRODUCTION

The hook shape reflectivity feature has been documented as an indicator of tornadoes [Fujita, 1958], however more than half of the tornadoes have been reported not associated with apparent hook signature. Tornado vortex signature (TVS) defined as the azimuthal velocity difference at a constant range is a parameter to quantify the tornado feature based on pulsed Doppler radar observation [Burgess et al., 1975]. The basic idea of the current tornado detection algorithm (TDA) is to search for strong and localized azimuthal shear in the field of mean radial velocities [e.g., Crum and Alberty, 1993; Mitchell et al., 1998]. However, because of the smoothing effect caused by the radar resolution volume, the shear signature can be significantly degraded if the size of tornado is small and/or the tornado is located at far ranges [Brown and Lemon, 1976]. Recently, a neuro-fuzzy tornado detection algorithm (NFTDA) has been developed by Wang et al. [2008] within atmospheric radar research center (ARRC) of the university of Oklahoma. Tornado shear signature and tornado spectral signatures (TSS) are combined in this algorithm, and the performance shows significant improvement. Conventionally, Weather Surveillance Radar-1988 Doppler (WSR-88D) provides legacy resolution with reflectivity data on a 1 km-by-1 ^{o} polar grid and Doppler data (radial velocity and spectrum width) on a 250 m-by-1 ^{o} grid. Super resolution proposed to be adopted by the WSR-88D can provide reflectivity data and Doppler data on a 250 m-by-0.5^o grid[e.g., Torres and Curtis, 2007]. The benefit of super resolution data can be fully realized through finer range and azimuthal sampling in conjunction with a narrower effective antenna pattern (i.e.,a smaller effective beamwidth) [Brown et al., 2002; Torres and Curtis, 2007]. Brown et al. [2002] have shown that tornado hook and vortex signatures can be more pronounced from super-resolution data. Tornado debris signatures (TDS) defined as high reflectivity (Z), anomalously low cross-correlation coefficient (ρ_{hv}) and very low (or negative) differential reflectivity (Z_{DR}) were first observed by Ryzhkov et al. [2005] using a S-band research polarimetric radar. Kumjian and Ryzhkov [2008] and Bluestein et al. [2006] further identified TDS during tornadic supercell storms using a S-band and a mobile X-band dual-polarization Doppler radar. The polarimetric upgrade of the WSR-88D network, supported by the National Weather Service (NWS), the Federal Aviation Administration (FAA) and Air Force Weather Agency is undergoing. With the polarimetric capability, the TDS can be incorporated into WSR-88D developing tornado detection algorithm. In this work, an advanced tornado detection algorithm using super-resolution and polarimetric data is proposed. The neuro-fuzzy framework is adopted by this advanced tornado detection algorithm, and the inputs parameters and rule inference are further modified. The performance of proposed algorithm is demonstrated using abundant real tornado cases. This paper is organized as follows. An overview of the upgraded NFTDA in section 2. The performance of the advanced NFTDA using legacy-, super-resolution and polarimetric data are evaluated in section 3. Finally, a summary and conclusions are given in section 4.

* *Corresponding author address:* Yadong Wang, University of Oklahoma, School of Electrical and Computer Engineering, University of Oklahoma, Norman, Oklahoma 73019; e-mail: wyd@ou.edu

2. UPGRADED NEURO-FUZZY TORNADO DETECTION ALGORITHM

2.1. Review of NFTDA

In the NFTDA developed by Wang et al. [2008], five parameters of velocity difference (Δv) spectrum width (σ_v), spectral flatness (σ_s), phase of the radially integrated bispectrum (P), and eigenratio (χ_R) are integrated by a fuzzy logic framework. Initially, the S-shape and Z-shape membership functions were used to convert the five crisp inputs into fuzzy membership degrees. Subsequently, a rule strength was set by the maximum of the product of the input fuzzy variables. The membership functions were initialized based on the results of statistical analysis, and fine-tuned through a training process with a neural network. The performance of NFTDA was demonstrated using Level I data collected by the research WSR-88D (KOUN) operated by the Na-

tional Severe Storms Laboratory (NSSL) during two tornadic events. These results show the performance of conventional TDA can be improved significantly using NFTDA in term of probability of detection (POD), false alarm ratio (FAR), critical success index (CSI), and maximum detection range.

2.2. Doppler moment based NFTDA (D-NFTDA) and polarimetric moment based NFTDA (P-NFTDA)

Although the original NFTDA has shown enhanced detection, three input parameters of σ_s, P and χ_R are derived from level I time series data which are not available for operational WSR-88D radar. In order to engage with operational products with the provision of polarimetric upgrade, the NFTDA has been modified to take in only Doppler moment data or polarimetric with Doppler moment data. Doppler moment data, specified as σ_v and Δv in this work, are the parameters incorporated into the Doppler moment based NFTDA (D-NFTDA). σ_v defined as second moments of a Doppler spectrum [Doviak and Zrnić, 1993], can be estimated using the periodogram method [Bringi and Chandrasekar, 2001], or autocovariance method [Doviak and Zrnić, 1993]. Δv is defined as velocity difference between two adjacent azimuthal gates. Since 99 % tornadoes in the northern hemisphere are cyclonic direction [Davies-jones, 1984], Δv is calculated using the radial velocity on higher azimuthal angle minus the lower one in this work. The TDS continently observed within tornadic storm can be a tornado indicator, especially when velocity and spectral signature is not obvious. The polarimetric with Doppler moment based NFTDA (P-NFTDA) which incorporates both TDS, σ_v and Δv, has potential in decreasing the FAR caused by velocity aliasing or nonvortex shear such as squall line.

2.3. Architecture of upgraded NFTDA

A schematic diagram is shown in Fig. 1 to demonstrate the working procedure of the upgraded NFTDA (including D-NFTDA and P-NFTDA). Three components of fuzzification, rule inference and defuzzification consist the fuzzy logic system. In fuzzification, S shape and Z shape membership functions are applied to the input parameters as in [Wang et al., 2008]. Input x_i can be specified as two (σ_v and ΔV) or four (σ_v, ΔV, Z_{DR} and ρ_{hv}) depending on the availability. Moreover, the input parameters can be in either Legacy or super resolution. Unlike the previous NFTDA, the rule inference has been modified to use weighted average instead of multiplication. The weighted average and multiplication can be thought of as "OR" and "AND" operation on those fuzzy inputs. Therefore when TDS or Doppler signatures are not existing simultaneously, using weighted average rule inference can still provide robust detection results, but multiplication is likely failed under this situation.

The output of NFTDA is a cluster of radar gates. Quality control (QC) procedure is implemented to eliminate the cluster associated with nonvortex azimuthal shear, such as gust fronts. If the aspect ratio, defined as the cluster's radial extent over azimuthal extent, exceeds a predefined threshold (set as four in this work), this cluster is discarded as an nonvortex cluster. The remained clusters are assumed associated with tornadic vortex, and the center of cluster which is designated to be the tornado center needs to be determined. In this work, the subtractive clustering method (SCM), an extension of the mountain clustering method proposed by Yager and Filev [1994] is used to finalize the vortex center. Unlike other clustering method such as fuzzy c-means (FCM) technique, which finds the cluster center with predefined cluster number, SCM can estimate the number of clusters and determine the clusters centers simultaneously. This advantage of SCM is especially important when more than one tornado presents in a given data set. In SCM, each data point is initially assumed to be a potential cluster center. Then a measurement of the likelihood that each data point would define the cluster center is calculated based on the density of surrounding data points. The data with highest potential is set as the first cluster center, and all the data points in the vicinity (as determined by a predefined radii) of the first cluster are removed. Iterating of this process until all of the data is within radii of a cluster center.

3. PERFORMANCE EVALUATIONS

In order to evaluate the performance of D-NFTDA, a library of tornado events with both radar data and tornado locations was established. 49 tornado events occurred during 1993 to 1999 for legacy resolution and 13 events during March 11^{th} 2008 to September 30^{th} 2008 for super resolution are currently included in this tornado library. The number and time period of tornadoes are based on the NCDC record (http://www4.ncdc.noaa.gov/cgi-win/wwcgi.dll?wwEvent Storms). All these tornadoes events are associated with: (1) the tornado's life time is more than 3 minutes, (2) the quality of radar data is sufficient and (3) all the tornadoes located within 150 km from the radar as suggested by Mitchell et al. [1998]. The corresponding WSR-88D Level II data were also obtained from the NCDC website

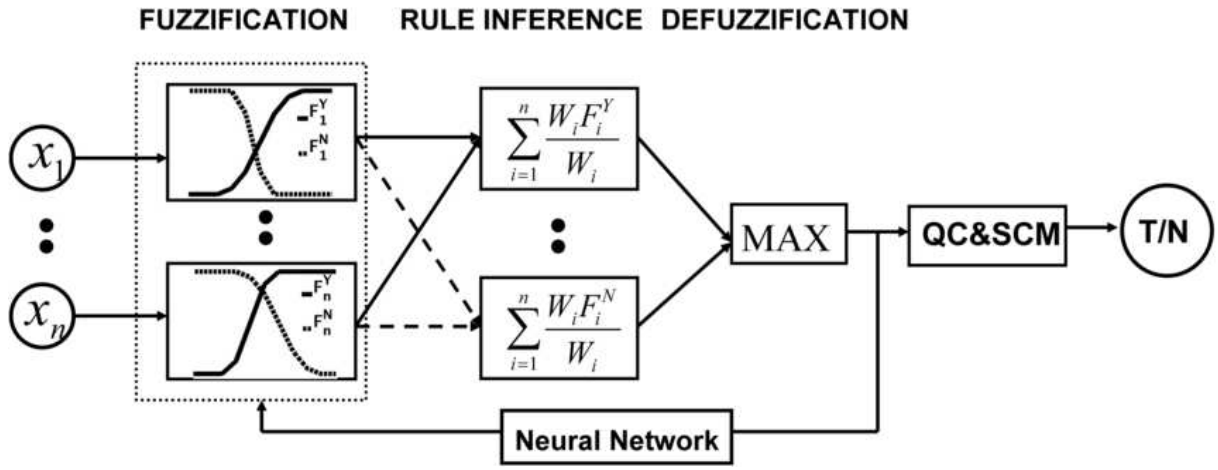

Figure 1: The schematic diagram of upgraded NFTDA. The framework is flexible enough to take in 2 or 4 parameters. n = 2 represents D-NFTDA, where spectrum width (σ_v) and velocity difference (ΔV) are two input parameters; n = 4 represents P-NFTDA, together with σ_v and ΔV, differential reflectivity (Z_{DR}), and cross correlation coefficient (ρ_{hv}) are the four inputs. A neural network is used to adjust the fuzzy logic membership functions, and the output of the neuro-fuzzy system is cluster of radar gates. Those gates associated with non-vortex are eliminated by quality control (QC), and the tornado center is determined using a subtractive clustering method (SCM).

(http://www.ncdc.noaa.gov/nexradinv/). Some of these cases were also used for the evaluation of the operational WSR-88D Tornadic Vortex Signature Detection algorithm (TDA) developed by NSSL [Mitchell et al., 1998]. In this work, the NSSL's Warning Decision Support System- Integrated Information (WDSSII) was used to produce TDA results [Lakshmanan et al., 2007], which will be used to compare with NFTDA detection.

3.1. D-NFTDA for legacy-resolution data

The 49 tornado events are divided into two groups for training and testing. The training groups is used to train the membership functions and the testing group is used to assess the performance. Parameters implemented in membership functions are initialized from statistical analysis, and further tuned with a neural network. Level II moments data from 9 tornado events associated with 21 volume scans are used in training the fuzzy logic membership functions. Various Fujita scales (F0 $\sim$ F3) tornadoes from close range (0 $\sim$ 50 km), median range (50 $\sim$ 100 km) and far range (100 $\sim$ 150 km) are included In the training data set, and listed in Table 1.

The location of a tornado associated with each radar volume scan was determined from the ground damage path when it is available. Otherwise, the tornado's starting, ending locations and the width of ground damage obtained from the storm report are used in helping determining the locations. These locations were further adjusted by carefully examining the location of hook-signature, strong azimuthal shear, and large spectrum width. Similar methodology of adjustment in time and/or location is also adopted by Mitchell et al. [1998] and Witt et al. [1998]. For each volume scan, a right detection defined as "hit" is obtained when the detection is within the close vicinity ($<$ 1 km) of the tornado right location. Other detections are defined as "false". In addition, a missed detection is obtained if the tornado is present but the algorithm produces no detection. To quantify the performance, the time window scoring method described in [Witt et al., 1998] was applied. Algorithms run within the time windows which starts from 15 minutes prior to the beginning time of the tornado to 5 minutes after the ending time of each tornado [Witt et al., 1998]. The time, location, radar, volume number, hit, miss, and false detection of each tornado events are itemized in Table 2. The POD, FAR, are defined by POD = $a/(a+c)$, FAR = $b/(a+b)$, , where a, b and c represent hit, false and miss, respectively.

The POD and FAR for D-NFTDA and NSSL's TDA are shown in Fig. 2 for different Fujita scales. It is evident that for weak tornadoes of F0-scale the D-NFTDA shows significant improvement from conventional TDA with much higher POD (from 6.7% to 47%) and lower FAR (from 91% to 30%). Moreover, the D-NFTDA can extend the detection range of F0 tornadoes from 36 km to approximately 60 km. For stronger tornadoes (F1-

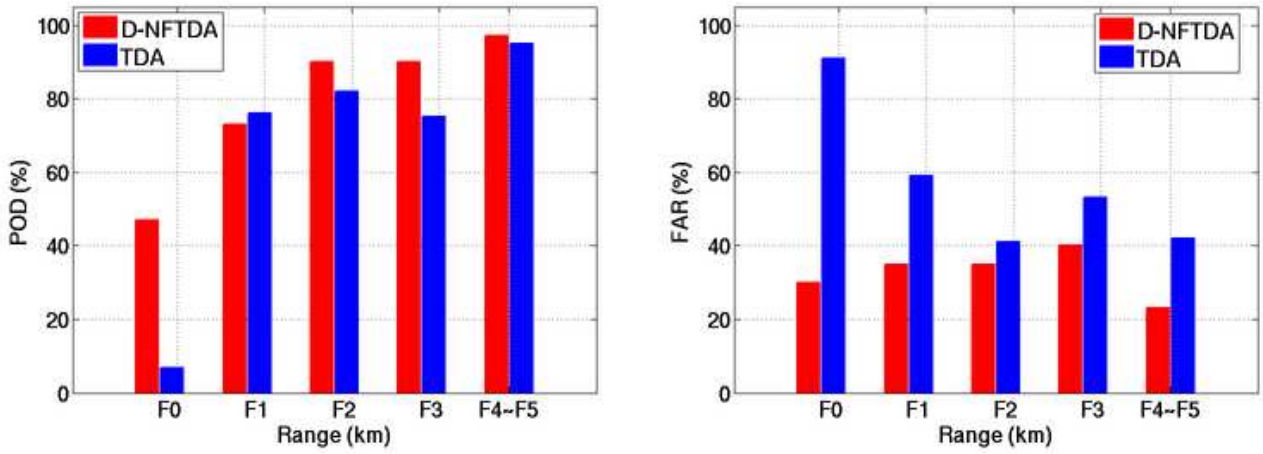

Figure 2: Statistical performance of POD (left) and FAR (right). The results are from 49 tornado events. The detection results of D-NFTDA are indicated by red bars, and the detections results of TDA generated by WDSSII are indicated by blue bars. The abscissa is the intensity of tornado in Fujita Scale.

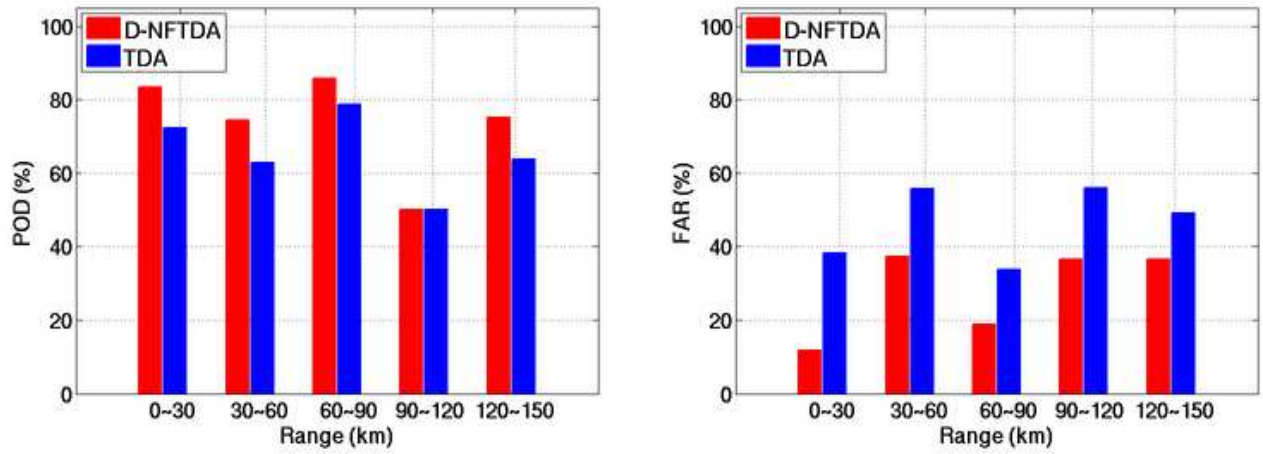

Figure 3: Similar as Fig. 2, but the abscissa is the distance from tornadoes to radars in very close range (0 $\sim$ 30 km), close range (30 $\sim$ 60 km), median range (60 $\sim$ 90 km), far range (90 $\sim$ 120 km) and very far range (120 $\sim$ 150 km).

Date	Radar	County, State	#Volume	Range (km)	Maximum EF-Scale
04/15/94	KLSX	St.Louis, MO	2	0–50	F0
10/07/96	KTBW	Tampa Bay Area, FL	2	50–100	F0
03/24/98	KHNX	Hanford, CA	5	100–150	F0
01/21/90	KLZK	Little Rock, AR	4	0–50	F2
07/03/90	KAPX	Gaylord, MI	1	50–100	F2
02/23/98	KMLB	Melbourne, FL	1	100–150	F2
05/31/96	KABR	Aberdeen, SD	1	0–50	F3
05/17/95	KDDC	Dodge City, KS	2	50–100	F3
02/23/98	KMLB	Melbourne, FL	3	100-150	F3

Table 1: Tornado events used in the training of D-NFTDA parameters for legacy-resolution data.

F5), the D-NFTDA offers comparable or slightly higher PODs compared to TDA. It is worth of noting that D-NFTDA has significantly lower FAR. For example, for F4 and F5 tornadoes, both algorithms produce comparable PODs of higher than 95%, but the NFTDA can more effectively suppress false detection to produce of FAR of 23%, while the FAR of TDA is 42%. The performance of D-NFTDA and TDA are also compared for different ranges, and the results are presented in Fig. 3.

Within the range of 150 km, D-NFTDA shows higher (or comparable) POD (83% vs. 72% at 0∼30 km, 74% vs. 62% at 30∼60 km, 85% vs. 78% at 60∼90 km, 50% vs. 50% at 90∼120 km and 75% vs. 63% at 120∼150 km) and lower FAR than TDA (11% vs. 38% at 0∼30 km, 37% vs. 55% at 30∼60 km, 18% vs. 33% at 60∼90 km, 36% vs. 55% at 90∼120 km and 36% vs. 49% at 120∼150 km).

3.2. D-NFTDA for super-resolution data

In this work, the membership functions are retrained using super-resolution data, and the performance of super-resolution version D-NFTDA is evaluated. For the purpose of evaluation, 13 tornado cases associated with Fujita scale from EF0 to EF3 with super-resolution moments were initially identified out of 1470 tornado cases achieved in the NCDC record from 11 March 2008 to 30 September 2008. Tornado life duration(longer than 3 minutes), distance to an available WSR-88D radar(less than 150 km) and data quality are the three criteria used in the data selection. Radar data from two volume scans on a F0 tornado case recorded by KFTG, and three volume scans on a F1 tornado case recorded by KDVN are used in the training procedure. Tornado cases used in testing are listed in Table 3.

Due to the limitation of available cases, tornadoes with Fujita scale of F0 and F1 are referred as week tornadoes and others are categorized as strong tornadoes. Moreover, the NSSL's WDSSII was used to simulate/convert Doppler moments from super resolution to the legacy resolution, which were then fed to the D-NFTDA and conventional TDA. The POD and FAR from the three approaches are presented in Fig. 4 For the legacy resolution, the D-NFTDA exhibits higher POD and lower FAR than TDA, which is consistent with previous results. It is interesting to note that for weak tornadoes the super-resolution D-NFTDA has enhanced POD of 75% and slightly decrease FAR of 33%, compared to the legacy D-NFTDA with POD of 60% and FAR of 28.3%.

3.3. P-NFTDA for legacy-resolution

An example is used to demonstrate the debris signatures within a tornado in Fig. 5. A tornado is indicated with a while circle, where apparent shear signatures, high value of σ_v, low value of Z_{DR} and ρ_{hv} can be observed. Similar values of σ_v and ΔV can also be found at approximately 4 km northeast of the circle. However, at the same location Z_{DR} and ρ_{hv} show apparent different value from the place associated with tornado. TDS becomes particularly important when a radar's ambiguous velocity is low, using C-band radar for example, which can not provide obvious tornado velocity and/or spectral signatures. Since current WSR-88D radars are upgrading into polarimetric model, even the P-NFTDA is only tested on research prototype radar, it has the potential to be implemented in future.

To demonstrate the capability of TDS in facilitating tornado detection especially in eliminating false detection, detection results from D-NFTDA and P-NFTDA on three tornadic events are compared, and the results are presented in Fig. 6.

			Number		Detection (NFTDA / TDA)		
Date	Radar	County, State	#Tornado	#Volume	Hit	Miss	False
05/31/96	KABR	Aberdeen, SD	1	29	7/5	3/5	4/7
05/22/95	KAMA	Amarillo, TX	1	10	1/2	0/1	0/1
07/03/99	KAPX	Gaylord, MI	1	13	4/4	0/0	0/0
05/21/98	KCYS	Cheyenne,WY	1	85	0/0	5/5	0/0
05/16/95	KDDC	Dodge City, KS	1	71	3/3	0/0	3/3
05/27/97	KEWX	Austin, TX	9	81	17/11	9/15	3/1
03/29/98	KFSD	Sioux Falls, SD	2	87	25/9	0/16	1/4
05/07/95	KFWS	Dallas/Fort, TX	2	41	12/8	5/9	3/1
05/12/95	KGLD	Goodland, KS	3	72	12/12	0/0	1/2
11/16/93	KHGX	Houston, TX	5	67	4/2	6/8	2/2
04/07/98	KILX	Lincoln, IL	4	137	6/6	5/5	2/3
01/02/99	KLCH	Lake Charles, LA	9	74	12/12	5/5	17/22
04/15/94	KLSX	St. Louis, MO	2	49	3/2	6/7	3/9
05/28/96	KLVX	Louisville, KY	2	33	13/13	1/1	4/10
03/29/98	KMPX	Minneapolis, MN	2	36	15/15	3/3	9/20
01/29/98	KNKX	San Diego, CA	1	12	0/0	5/5	0/0
04/03/99	KSHV	Shreveport, LA	1	32	12/11	9/10	7/17
09/02/98	KTBW	Tampa Bay, FL	2	45	5/4	8/9	1/0

Table 2: Tornado events used in the testing of D-NFTDA parameters for legacy-resolution data.

			Number		Detection (NFTDA / TDA)		
Date	Radar	County, State	#Tornado	#Volume	Hit	Miss	False
07/02/08	KDMX	Des Moines, IA	1	25	3/3	6/6	3/3
07/10/08	KDVN	Davenport, IA	2	14	7/0	7/14	8/2
08/24/08	KFTG	Denver, CO	1	9	0/0	6/6	0/0
06/04/08	KIND	Indianapolis, IN	2	14	8/6	2/4	6/10
07/14/08	KLNX	North Platte, NE	2	14	4/0	8/12	0/0
08/02/08	KLWX	Sterling, VA	2	14	4/0	8/12	0/0
05/08/03	KOUN	Norman, OK	1	6	2/0	0/2	2/3
05/10/03	KOUN	Norman, OK	3	12	9/5	0/4	2/3

Table 3: Tornado events used in the testing of D-NFTDA parameters for super-resolution data.

These three events occurred on center Oklahoma on 10 May 2003, and radar data are recorded using research prototype polarimetric radar WSR-88D KOUN. Detail damage path from ground survey is available which inserted in Fig. 6 as one reference. Both D-NFTDA and P-NFTDA can detect the tornado all the time, except two false detections at 03:41 and 03:47 from D-NFTDA existing on the north of the damage path. The velocity at these two moments are presented in Fig. 6, from where obvious velocity aliasing can be observed. False detections come out if they are not/incorrectly dealiasing. However, ρ_{hv} and Z_{DR} does not show obvious low value at these two locations, and no TDS can be identified. Therefore, even large velocity difference and spectrum width can be observed, they still can be eliminated.

4. SUMMARY AND CONCLUSIONS

The enhanced detection capability of original NFTDA has been shown through simulation results and real cases analysis. However, three parameters σ_s, P and χ_R defined as tornado spectral signature (TSS), are derived from level I time series data, which are not available for current operational WSR-88D radar. In order to engage with operational products and increase the commercial value of the algorithm, the NFTDA needs to be modified to take in parameters available currently or in future. Advanced neuro-fuzzy tornado detection algorithm is developed in this work. Through the evaluation on the real tornado events, the performance of this Advance tornado detection algorithm shows significant improvement. Even more, the performance using

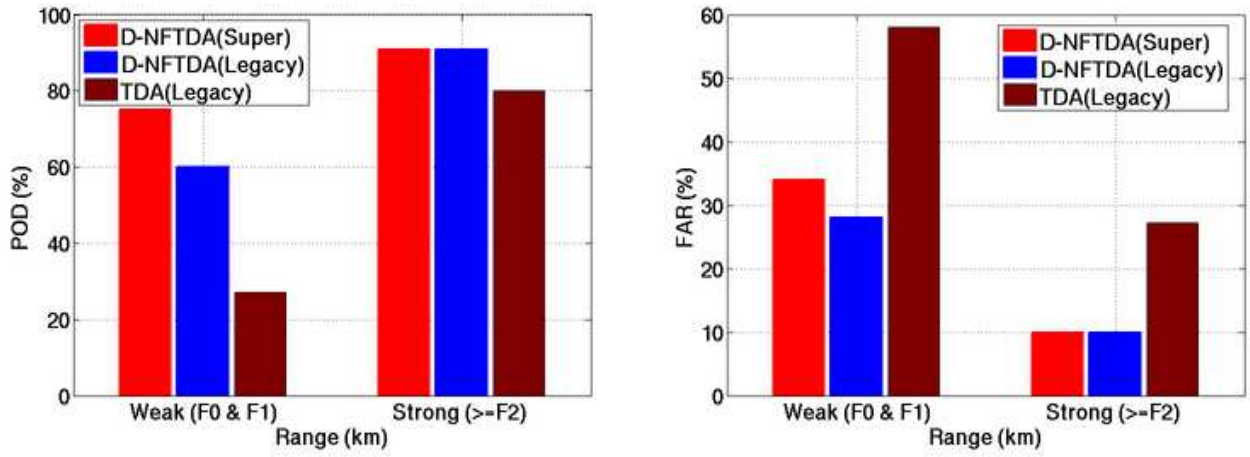

Figure 4: Similar as Fig. 2, but for super resolution data.

super-resolution data shows further improvement than legacy resolution data. With the incorporation of polarimetric data, false detections caused by nonvortex shear, such as velocity aliasing can be eliminated.

5. ACKNOWLEDGMENT

This work was supported by the Enterprise Electronics Corporation (EEC) and WSI Corporation under the project of advanced tornado detection. The authors would also like to thanks the NSSL staff for the collection of Level I data.

References

Bluestein, H. B., M. M. French, and L. R. Tanamachi, 2006: Close-range observations of tornadoes in supercells made with a dual-polarization, X-band, mobile Doppler radar. *Mon. Weather Rev.*, **135**, 1522–1543.

Bringi, V. N., and V. Chandrasekar, 2001: *Polarimetric Doppler Weather Radar Principles and Applications*. Cambridge University Press, Cambridge, UK.

Brown, R. A., and L. R. Lemon, 1976: Single Doppler radar vortex recognition. part ii: Tornadic vortex signatures. *Prepr. Radar Meteor. Conf.*, **104-109**.

Brown, R. A., L. R. Lemon, and D. W. Burgess, 1978: Tornado detection by pulsed Doppler radar. *Mon. Weather Rev.*, **106**, 29–38.

Brown, R. A., V. T. Wood, and D. Sirmans, 2002: Improved tornado detection using simulated and actual WSR-88D data with enhanced resolution. *J. Atmos. Oceanic Technol.*, **19**, 1759–1771.

Burgess, D. W., L. R. Lemon, and R. A. Brown, 1975: Tornado characteristics revealed by doppler radar. *Geophys. Res. Lett.*, **183-184**.

Crum, T. D., and R. L. Alberty, 1993: The WSR-88D and the WSR-88D operational support facility. *Bull. Amer. Meteor. Soc.*, **74**, 1669–1687.

Davies-jones, R., 1984: Streamwise vorticity: the origin of updraft rotation in supercell storm. *J. Atmos. Sci.*, **20**, 2991–3006.

Doviak, R. J., and D. S. Zrnić, 1993: *Doppler Radar and Weather Observations*. Academic Press, San Diego, Calif., 130 pp.

Fujita, T., 1958: Mesoanalysis of the illinois tornadoes of 9 April 1953. *J. Atmos. Sci.*, **15**, 288–296.

Kumjian, M. R., and A. V. Ryzhkov, 2008: Polarimetric signatures in supercell thunderstorms. *J. Appl. Meteorol.*, **47**, 1940–1961.

Lakshmanan, V., T. Smith, G. J. Stumpf, and K. Hondl, 2007: The warning decision support system - integrated information (WDSS-II). *Wea. Forecasting*, **22**, 592–608.

Mitchell, E. D., S. V. Vasiloff, G. J. Stumpf, A. Witt, M. D. Eilts, J. T. Johnson, and K. W. Thomas, 1998: The National Severe Storms Laboratory tornado detection algorithm. *Wea. Forecasting*, **13**, 352–366.

Ryzhkov, A. V., T. J. Schuur, D. W. Burgess, and D. S. Zrnic, 2005: Polarimetric tornado detection. *J. Appl. Meteorol.*, **44**, 557–570.

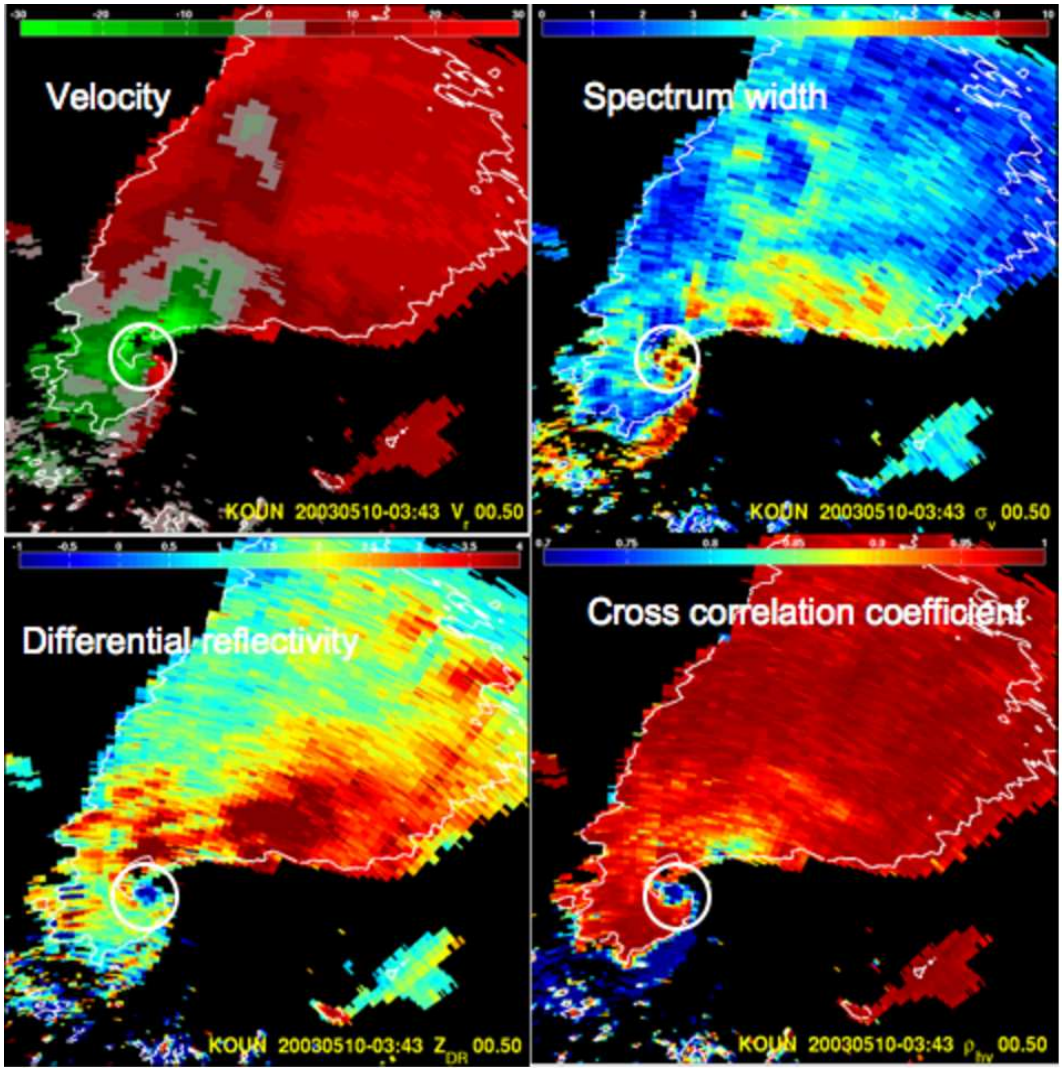

Figure 5: The Doppler velocity (top left), σ_v (top right), Z_{DR} (bottom left) and ρ_{hv} (bottom right). Tornado location is indicated by a white circle, and reflectivity with 30 dB is indicated using white contour.

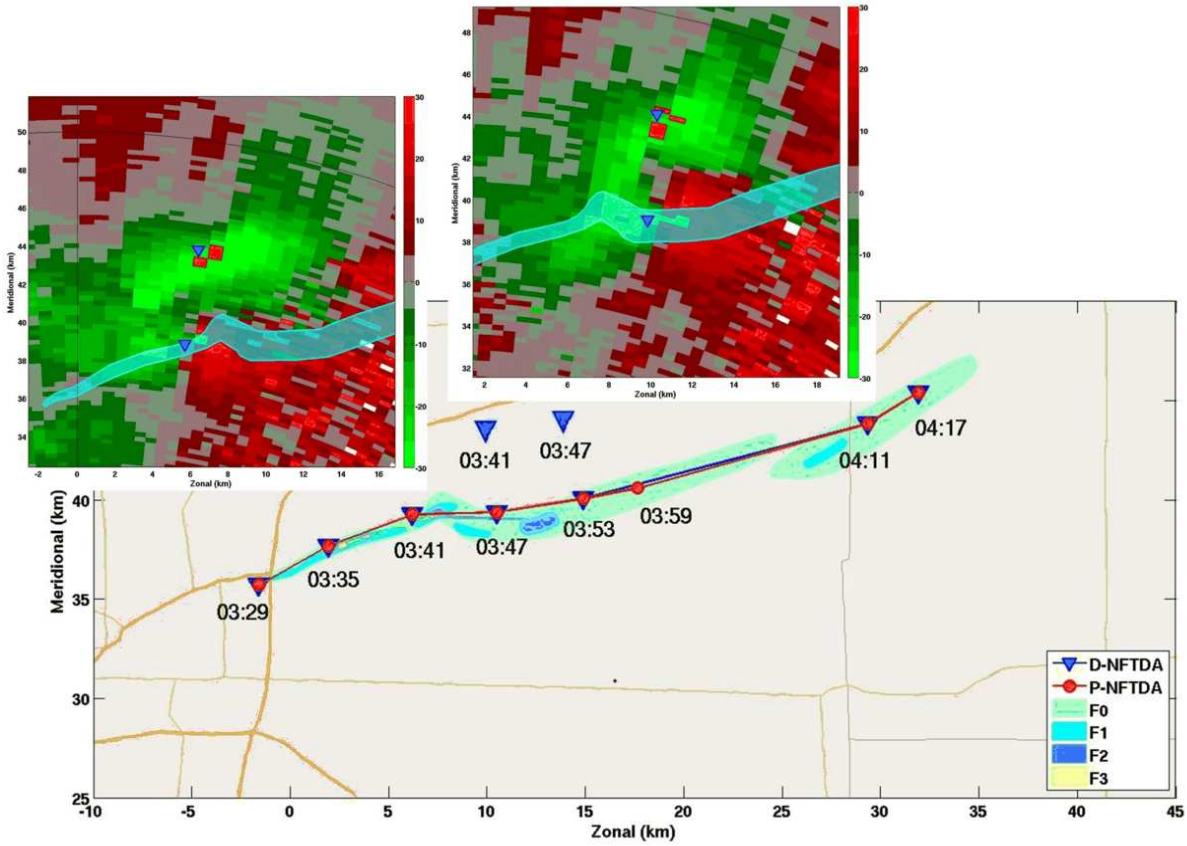

Figure 6: Comparisons of the detection results from D-NFTDA and P-NFTDA, which are denoted by blue triangles and red circles respectively, for tornadoes on 10 May 2003.The detection of ”hit” from each approach is connected by a solid line to show the time continuity. Ground damage path with Fujita scales are depicted by color-shaded contours. The Doppler velocity plot at 03:41 and 03:47 are inserted. False detection at these two moments are 3, 4 km away from the damage path, respectively.

Torres, S. M., and C. D. Curtis, 2007: Initial implementation of super-resolution data on the NEXRAD network. in *23th Conference on interactive information processing systems (IIPS) Ffor meteorology, oceanography, and hydrology*. AMS.

Wang, Y., T.-Y. Yu, M. Yeary, A. Shapiro, S. Nemati, M. Foster, and J. D. L. Andra, 2008: Tornado detection using a neurofuzzy system to integrate shear and spectral signatures. *J. Atmos. Oceanic Technol.*, **25**, 1136–1148.

Witt, A., M. D. Eilts, G. J. Stumpf, E. D. Mitchell, J. T. Johnson, and K. W. Thomas, 1998: Evaluating the performance of WSR-88D severe storm detection algorithms. *Wea. Forecasting*, **13**, 513–518.

Yager, R., and D. Filev, 1994: Generation of fuzzy rules by mountain clustering. *J. Intelligent Fuzzy Sys.*, **2**, 209–219.